CrossMark

ORIGINAL PAPER

Inter- and intraannual growth patterns of urban small-leaved lime (*Tilia cordata* mill.) at two public squares with contrasting microclimatic conditions

Astrid Moser[1] · Mohammad A. Rahman[2] · Hans Pretzsch[1] · Stephan Pauleit[2] · Thomas Rötzer[1]

Abstract The effects of urban conditions on tree growth have been investigated in an increasing number of studies over the last decades, emphasizing the harsh environment of cities. Urban trees often grow in highly paved, compacted sites with consequently less soil moisture, higher soil temperatures, and greater vapor pressure deficits. However, there is still a knowledge gap regarding the impact of harsh paved environments on urban tree growth during drought years on the growth patterns of urban trees. The present study investigated the structure and growth of the common urban tree species small-leaved lime (*Tilia cordata*) at a highly paved public square (CPS) compared with a contrasting more open, greener square (OGS). Continuously, measured high precision dendrometer data along with meteorological data of the extreme dry and warm summer 2015 as well as dendrochronological data of the sampled trees were investigated to analyze tree growth during a drought year. The results highlight different tree dimensions and growth patterns of the trees at both sites, influenced by tree age and distinct site conditions. While the trees at OGS grew up to 2.5 mm from July until mid of August, the trees at CPS had only 0.4-mm diameter increment. After the initial expansion at CPS, tree diameter contracted again during summer to the point of shrinkage (up to 0.8 mm) at the end of our investigation. Further drought year analysis confirmed the patterns of significant stem growth reductions in the consecutive two years following the drought. A correlation analysis revealed that transpiration, air temperature, and vapor pressure deficit were negatively correlated with the daily diameter growth, whereas precipitation had a strong positive effect. Due to high transpiration rates associated with anisohydric water use behavior, *T. cordata* was able to provide evaporative cooling even during drought. However, this anisohydric behavior resulted in substantial growth decline afterwards especially at paved sites like CPS. Our results suggest selection of tree species, such as those with isohydric water use behavior, which may achieve a better balance between growth, transpiration, and hence evaporative cooling.

Keywords Drought stress · Microclimate · Tree growth · Urban trees

Introduction

Compared to forest stands, urban trees grow in harsh environments with limited rooting space (Day et al., 1995), high temperatures (Kim, 1992; Day et al., 2010), less access to soil moisture and nutrients (Kjelgren and Clark, 1992; Rhoades and Stipes, 1999), and reduced aeration due to impervious pavement (Morgenroth and Buchan, 2009; Rahman et al., 2013). During the past decades, many studies analyzed the effects of growth conditions on urban tree growth and mortality (Nowak et al., 1990; Kjelgren and Clark, 1992; Hodge and Boswell, 1993; Gregg et al., 2003). For example, Bühler et al. (2007) and Day et al. (1995) reported that the planting methods and pit sizes are of great importance for tree establishment and vitality. Species sensitive to soil compaction with sparse rooting space showed reduced growth and vitality

✉ Astrid Moser
astrid.moser@lrz.tum.de

1   Chair for Forest Growth and Yield Science, School of Life Sciences Weihenstephan, Technische Universität München, Hans-Carl-von-Carlowitz-Platz 2, 85354 Freising, Germany

2   Chair for Strategic Landscape Planning and Management, School of Life Sciences Weihenstephan, Technische Universität München, Emil-Ramann-Str. 6, 85354 Freising, Germany

(Sjöman et al., 2015). Altogether, the mentioned growth conditions can lead to an enhanced soil moisture stress for urban trees.

Water availability can be the most important determinant of tree growth (Littell et al., 2008; Allen et al., 2010; Zhao and Running, 2010; Williams et al., 2013). Along with less water availability during summer, especially in drought years, strong atmospheric demands might drive more transpiration exceeding the tree's water uptake (Clark and Kjelgren, 1990). This negative water balance can result in an internal water deficit in the tissues. Planting drought tolerant species is a possible adaption strategy to water shortage (Moser et al., 2016). Different drought tolerant species usually illustrate different adaption strategies against drought such as early leaf loss (Tyree et al., 1993; Sandquist and Ehleringer, 1998), closure of stomata (Gallé et al., 2007; Pretzsch et al., 2014), osmotic adjustment (Elmi and West, 1995; Arndt et al., 2000), alteration of leaf orientation (Comstock and Mahall, 1985; Werner et al., 1999), and reduction in leaf area (Liu and Stützel, 2004). Among them, different strategies concerning the water use behavior have been commonly discussed, resulting in two different types of adaptation: isohydric species close their stomata immediately during a drought event versus anisohydric species, which are characterized by a slower closure of stomata during and after drought (Pretzsch et al., 2014; Río et al., 2014). Further, the stomatal regulation of isohydric species maintains a consistent minimum leaf water potential, while the leaf water potential of anisohydric species markedly decreases with changes in evaporative demands (Klein, 2014).

Different tree species and even trees of same species but growing in distinct site conditions with different nutrient and soil moisture availability can show altered growth and vitality (Kjelgren and Clark, 1992). Nonetheless, few studies have investigated the effects of the urban climate on tree water relationships and the water balance of typical species in relation to their ecophysiology and hydric behavior (Bush et al., 2008; Chen et al., 2011).

Apart from harsh growth conditions, urban areas are characterized by huge microclimatic differences within short distance depending on the structure of the sites. Urban trees are commonly planted in street canyons, plazas, pedestrian areas, parking areas, and industrial areas (Ko et al., 2015). Those sites combined are regarded as paved urban area impervious to water infiltration and vapor, providing unique surroundings and microclimates for urban trees concerning radiation, water availability, soil compaction, evaporative demands, physical and rooting space, and light availability (Kjelgren and Clark, 1992). While in parks, these extreme conditions are less pronounced and street trees are exposed to high levels of radiation and water shortage with limited rooting space. Kjelgren and Clark (1992) analyzed the microclimatic characteristics of three typical urban environments, street canyons, parks, and plazas, and the effects on the ecophysiology and

growth of mature *Liquidambar styraciflua* trees. Differences in radiation, air temperature, vapor pressure deficit, and evaporation between the sites were found, with the highest values at plazas resulting in the least tree vitality and growth due to higher evaporative demands and limited soil resources (Dobbertin, 2005).

Consequently, tree species with different drought tolerances and ecophysiological traits can have different growth patterns as influenced by their surrounding above—and belowground environment. Still, there is a knowledge gap regarding the growth of mature trees at contrasting urban conditions based on detailed measurements of tree growth, ecophysiological parameters, and micrometeorological conditions especially in relation to climate change and drought. For example, Kjelgren and Montague (1998) investigated the stomatal response and transpiration of *Pyrus calleryana* trees grown over different surfaces. However, the study was conducted with young trees (height of 2.5 m) in containerized pots. With older and larger trees as well as under changed climatic scenarios with frequent years of low precipitation and high temperatures, those results might be substantially different. Knowledge about tree vitality and tree growth in urban street canyons—especially during drought summers—is of special importance for arborists and urban planners since trees provide numerous benefits for the amelioration of the microclimate and well-being of humans (Dimoudi and Nikolopoulou, 2003; Dobbs et al., 2014). A mechanistic understanding of the relationships between tree growth and environmental parameters can provide input for dynamic modeling of urban trees' carbon sequestration (Nowak and Crane, 2002) as well their capacity for cooling by evapotranspiration and shading (Akbari et al., 2001; Shashua-Bar and Hoffman, 2003). Currently, estimates of carbon sequestration and storage are mostly based on static assumptions (Nowak and Crane, 2002; Yoon et al., 2013). Especially, the cooling ability is of great importance for the city climate and human comfort, which has been intensively researched during the past years (McPherson et al., 1997; Gill et al., 2007; Rahman et al., 2015). Due to the difficulties in measuring, scarce data are available on the evapotranspiration of urban trees in relation to their growth and site conditions (water availability, surface temperature, wind speed) and their vitality (trees with less drought resistance have higher evapotranspirational water loss and provide less cooling) (Rahman et al., 2014, 2015). With impending climate change scenarios (IPCC, 2007), the services of trees for the city climate are getting more and more attention and urban trees will play a key role for climate adapted cities (Tyrväinen et al., 2005). The growing conditions influence the vitality and growth of urban trees (Bühler et al., 2006): Stress caused by water deficits reduces photosynthetic productivity and tree growth (Pretzsch and Dieler, 2011; Rötzer et al., 2012), at worst resulting in early senescence (Clark and Kjelgren,

1990). Vital trees are expected to grow faster and provide more benefits for the urban climate (Gómez-Muñoz et al., 2010; Sjöman et al., 2015). However, how common urban tree species react to changed climatic conditions in relation to their site conditions is still scarcely known.

The present study aims to improve the understanding of the growth patterns of urban trees at different urban sites under present climatic conditions as well as in respect to potential climate change and drought years. Therefore, we investigated the commonly planted urban tree species *Tilia cordata*, located at two contrasting sites within the center of a major city (Munich). To address the mentioned knowledge gaps about the growth of urban trees and the effects of the present growth conditions on tree vitality and benefits, we posed the following questions: (1) Do *T. cordata* trees grow differently when planted at two contrasting sites in terms of the degree of impervious surface (highly paved site compared to open, greener site)? (2) How do the reaction patterns to drought stress differ between the chosen contrasting environments? (3) What are the main driving forces behind the revealed growth reaction patterns of urban trees in relation to the microclimate?

Material and methods

Site description and data collection

The study site Munich is the third largest city in Germany, located close to the Alps and characterized by a warm temperate climate. The long-term (1961–1990) annual precipitation mean is 959 mm, whereas the mean annual temperature is 9.4°C (DWD, 2016). Munich shows a strong UHI effect with monthly mean UHI intensity up to 6°C in the city center (Pongracz et al., 2010). Two sites within the city center were chosen for data collection, representing typical urban conditions: Bordeaux Platz is an open, green square with less pavement (OGS), while the Pariser Platz is likely to be a highly compacted, heavily paved square (CPS) (Fig. 1). Our criteria for site selection were as follows: (1) two sites with contrasting characteristics in terms of micrometeorology and surface cover, (2) commonly planted and healthy matured street trees of the same species in a sufficient number, and (3) situated close to the city center with pronounced urban heat island (UHI) effect.

Both sites are situated close together (distance of 180 m), with OGS being far bigger than paved-CPS (17,250 to 1945 m²). CPS is a roundabout connected by six roads with heavy traffic with 10 *T. cordata* trees planted, while green-OGS is an oval-shaped avenue with two roads going in opposite directions with less traffic and 84 *T. cordata* trees in total. In total, ten trees at both sites were chosen for data collection. At OGS, we selected five trees of the most southern side, while at CPS we selected five neighboring trees in S, SW,

W, NW, and N directions. The average size of the uncovered tree pit is 55 m² at OGS and 5.8 m² at CPS. The planting pits of OGS are avenue plantations surrounded by lawn while the planting pits at CPS are small cut-out pits. Both sites were contrasting in terms of micrometeorological differences especially regarding wind speed and direction due to the shape of the canyons. Paved-CPS had lower wind speed, showed more channeling effect compared to OGS.

We investigated growth patterns, ecophysiology, and drought response of *T. cordata* trees at each site with high precision dendrometer data and increment core data. *T. cordata* was chosen for investigation since it is a commonly planted urban tree species (Pauleit et al., 2002); it is characterized as a shade-tolerant species (Radoglou et al., 2009). Tree data was collected from June to October 2015. The following tree information was recorded: diameter at breast height (dbh), tree height, height to live crown base, crown diameter, crown projection area (CPA), open surface area of the tree pit (OSA), vitality, coordinates including altitude, as well as the leaf area index LAI. Tree height was measured using a Vertex Forestor. The crown radius and the OSA of each tree were measured in eight intercardinal directions (N, NE, ..., NW) along the ground surface from the center of the trunk to the tip of the most remote downward-projecting shoot and to the last visible open, non-asphalted surface of the soil, respectively, according to Moser et al. (2015, 2016). LAI was estimated from hemispherical photographs taken during the fully leafed phase (June–August) using a Nikon Coolpix P5100 camera with fisheye lens and Mid-OMount following Moser et al. (2015). The resulting hemispherical photos were processed with the program WinSCANOPY (Régent Instruments Inc., Quebec, Canada). Among several methods, we used the LAI-2000 generalized method based on the work of Miller (1967) and Welles and Norman (1991) for deriving LAI.

Meteorological data collection

Air temperature, air pressure, relative air humidity, precipitation, wind speed, and direction were measured with two Vaisala Weather Transmitters WXT520 (EcoTech Umwelt-Meßsysteme GmbH, Bonn, Germany) at OGS and CPS. The stations were installed on top of street lamp posts at a height of 3.3 m by cross arms 2 m outward from the lamp to avoid influence of lamp and shade of the nearby trees and buildings (Rahman et al., 2017). At OGS, the weather station was placed in a straight line 16.8 m away from the first tree and at CPS 11 m away right at the center of the site to capture differences in micrometeorology as accurately as possible. All measured data were recorded continuously in a 15-min resolution from July 28th to October 21st 2015 on a enviLog remote data logger (EcoTech Umwelt-Meßsysteme GmbH, Bonn, Germany) at each site (Rahman et al., 2017).
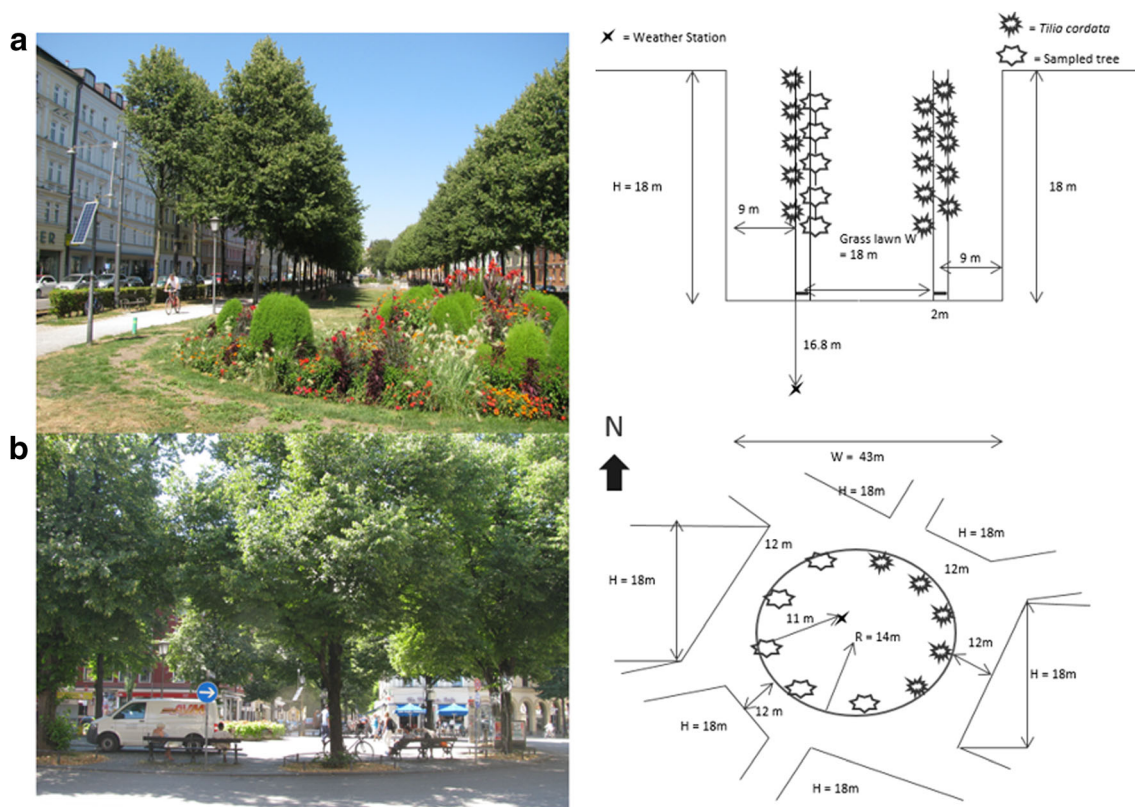
Fig. 1 Illustrations of Bordeaux Platz (open green square OGS) (**a**) and Pariser Platz (compacted paved square CPS) (**b**) in Munich

Soil moisture potential and temperature measurements

Soil matric potential and temperature were measured using Tensiomark 1 (4244/1, range pF 0-pF 7) (EcoTech Umwelt-Meßsysteme GmbH, Bonn, Germany) installed vertically through the soil profile to a depth of 30 cm. At OGS, the sensors were installed 3.5 m away from the main stem within the edge of the CPA. Three sensors were installed at the first tree, followed by two sensors for the next four to have three replicates for each tree within the grass verges. At CPS, a different setting was necessary due to the small planting pits. Here, two sensors for each tree were installed at the furthest opening point from the main stem. All the sensors were installed where shade was the heaviest to minimize the effect of direct radiation on the soil surface (Rahman et al., 2017).

Growth data collection in 2015—dendrometer

For continuous measurements of stem growth, precision dendrometer (Ecomatic, Dachau, Germany) was attached at approximately 4-m height at five trees of each site. The dendrometer measures the linear shifting of a small sensing rod fixed at the bark of the trunk. With stem contraction and expansion, the rod is displaced as well, translating the movement in an electrical signal (Mäkinen et al., 2008; Drew and Downes, 2009). Raw data were recorded every 5 min from

June 23rd to October 21st 2015 and stored in a CR800 data logger (Campbell Scientific, U.K.) equipped with Campbell Logger Multiplexer (AM16/32B). The height was chosen to ensure inaccessibility of installed devices to avoid vandalism.

Growth over time: dendrochronology

At both sites, from the five *T. cordata* we studied in detail and of five additional trees each, two cores opposite to each other were extracted at a height of 1.3 m in northern and southern directions. The obtained cores were processed by mounting on grooved boards with glue and sanded using progressively finer sand papers. The first sanding was conducted to flatten the increment cores while the subsequent sandings polished the cores to improve visualization of the cross-sectional area (Speer, 2012). The annual tree ring widths of the cores were measured with a Lintab digital positioning table with a resolution of 1/100 mm (Rinn, 2005). For cross-dating of the time series, the software packages TSAP-Win (Rinn Tech, 2010) were used. All following analyses were carried out with R (R Core Team, 2014), package dplR (Bunn et al., 2015). The tree ring series were detrended with a double detrending process, applying modified negative exponential curves and cubic smoothing splines (20 years rigidity, 50% wavelength cutoff, further averaged with Tukey's biweight robust mean. The autocorrelation of every series was removed using

autoregressive models (maximum order of 3). All further analyses of climate-growth correlations were conducted with the resulting chronologies. The statistical validity of the chronologies was assessed by the Expressed Population Signal (EPS) for the common period of the series. The EPS quantifies the degree to which the final chronology represents the hypothetically perfect chronology (Briffa and Jones, 1990). From the chronologies, the age of the analyzed trees was derived. If the exact age of the tree was not clear (missing tree pith etc.), the age was back-calculated based on the undetrended average growth rate of the last 10 years and the dbh of the tree.

Further, a pointer year analysis was conducted; it computes the individual relative radial growth variation by comparing the ring width of year t to that of year $t-1$ for each tree's chronology. The sign and magnitude of the found variation between the series were calculated (Mérian and Lebourgeois, 2011; Bunn et al., 2015). Positive pointer years display an extraordinary wide ring width, while negative pointer years are characterized by exceptionally narrow rings appearing concurrently within the analyzed trees (Gillner et al., 2014). In this study, pointer years were defined as those years where at least 75% of the series presented an absolute relative radial growth variation higher than 10% (Bunn et al., 2015).

Climate-growth relationships

To investigate the effects of climate on tree growth, we calculated a monthly drought index, the SPEI (Vicente-Serrano et al., 2010), using data of DWD (2016). The SPEI uses precipitation and potential evapotranspiration (PET) as input data (Vicente-Serrano et al., 2010), whereby a monthly PET was calculated according to the Penman-Monteith equation (Allen et al., 1998) including monthly mean daily minimum and maximum air temperature in °C instead of ambient vapor pressure, monthly mean wind speed in km/h and monthly mean sunshine hours in h. Using the calculated SPEI, the influence of the identified drought years on the growth patterns of urban trees was investigated. A yearly SPEI for 1985–2015 was computed by averaging the monthly index values of the growing season from April to September. Years with an SPEI smaller than −1 were classified as moderate drought years, whereas years with an SPEI smaller than −2 were interpreted as years with severe droughts (Lough and Fritts, 1987; Vicente-Serrano et al., 2010).

Moreover, we analyzed the influence of drought years on tree growth by using a superposed epoch analysis (SEA). SEA assesses the significance of events like droughts on tree growth during drought and post-drought growth periods (Bunn et al., 2015). Following Lough and Fritts (1987), Orwig and Abrams (1997), and Gillner et al. (2014), deviations from the mean ring width index of each core were calculated for the following two periods. The growth of each tree during the drought year derived by the SPEI and the growth of each tree during the 5 years after the drought year (post-drought) were averaged to detect significant departures between those superposed epochs.

Statistical analysis

All data analysis was conducted with R (R Core Team, 2014). Two-sample t tests were applied to check for statistical differences regarding the tree dimensions of the selected trees at both sites. Assumptions on normal distribution of data and homogeneity of variances were given.

Data derived by dendrometer were cleared of error values (e.g., touching the dendrometer during installation). Dendrometer displacement was converted in micrometer, and daily diameter growth curves were developed for each tree. To assess the influence of measured meteorological data on tree growth in 2015, daily growth values of dendrometer were analyzed in respect to meteorological values via Spearman's rank correlation tests. Further, using the R package mgcv a generalized additive mixed model (GAMM) with daily tree growth over time related to the sites and the meteorological data was developed.

The pointer year analysis and the SEA were computed using the R package dplR (Bunn et al., 2015). For the SEA, random sets of 11 years from 10,000 bootstrapped sets (Gillner et al., 2014; Bunn et al., 2015) were applied.

Results

Structure of *T. cordata* at Bordeaux Platz and Pariser Platz

Tree dimensions age, dbh, tree height, crown radius, crown length, CPA, and crown volume of the analyzed trees were significantly higher for trees grown at CPS compared with OGS along with significantly higher age (Table 1). However, open surface area (OSA) was significantly lower at CPS than at OGS. Although LAI of trees at CPS was higher than those of the trees at OGS, they were not significantly different.

Interannual growth patterns and climate–growth relationships

Due to the younger age, the growth rate of the trees at OGS was 5.0 mm year^{-1} and markedly higher than that of CPS (2.6 mm year^{-1}) (Table 2). By contrast, basal area increment (BAI) of trees at CPS was higher compared to those at OGS (206.7 to 80.5 mm^2 year^{-1}) (Table 3). Moreover, the investigated trees at OGS showed a slightly higher mean growth sensitivity than CPS. Both detrended chronologies exceed

Table 1 Minimum, average and maximum age, stem diameter (dbh), and tree height (a), crown radius, crown length, and crown projection area (CPA) (b), crown volume, open surface area (OSA), and leaf area index (LAI) (c) of *Tilia cordata* at Bordeaux Platz (open green square OGS) and Pariser Platz (completely paved square CPS), n = sample size

(a)

Site	n	Age [year]			Dbh [cm]			Tree height [m]		
		Min	Mean[1]	Max	Min	Mean[1]	Max	Min	Mean[1]	Max
Green-OGS	10	35	43[a]	49	25.8	28.7[a]	30.3	13.7	14.9[a]	15.6
Paved-CPS[2]	10	67	95[b]	132	37.7	44.1[b]	50.6	15.9	17.3[b]	19.2

(b)

Site	n	Crown radius [m]			Crown length [m]			CPA [m^2]		
		Min	Mean[1]	Max	Min	Mean[1]	Max	Min	Mean[1]	Max
Green-OGS	10	4.0	4.6[a]	5.0	9.0	10.5[a]	11.9	50.9	61.8[a]	79.3
Paved-CPS	10	4.8	5.1[b]	5.5	12.2	13.8[b]	14.8	72.6	82.5[b]	95.8

(c)

Site	n	Crown volume [m^3]			OSA [m^2]			LAI [m^2 m^{-2}]		
		Min	Mean[1]	Max	Min	Mean[1]	Max	Min	Mean[1]	Max
Green-OGS	10	463.1	655.9[a]	895.8	30.2	55.2[a]	48.7	1.8	2.4[a]	3.9
Paved-CPS	10	965.1	1135.5[b]	1341.9	6.2	5.8[b]	8.7	2.0	2.6[a]	3.9

[1] Mean values in the same column differ significantly when followed by different letters (Two-sample t-test, $p < 0.05$)

[2] Age of CPS based on extrapolated values

the commonly applied threshold of 0.85 for the EPS (Wigley et al., 1984).

The time series of trees at CPS covered the period of 1926 to 2015 while the time series of trees at OGS ranged from 1987 to 2015 (Fig. 2). In general, the trees at both sites displayed similar growth patterns with low growth episodes e.g., in 2005 and high growth episodes e.g., in 2007.

To statistically validate the years with extreme low and high growth, a pointer year analysis was conducted (Table 3). Pointer years at both sites were found for 2005, 2009, and 2011. Other years like 2003 are negative pointer years at only one of the investigated sites. All in all, eight negative pointer years were found for green-OGS and nine for paved-CPS. In the common time period of both sites, less positive pointer years (8) were found at CPS compared to OGS (9). Similar patterns were found regarding the negative pointer years of both sites (6 at CPS and 8 at OGS).

Using the SPEI, the growth of *T. cordata* at both sites before, during, and after drought years was investigated (Fig. 3). In Munich, the SPEI of the worst drought year (2003) was −1.8, other drought years were 2015 (−0.75), 2014 (−0.80), 2004 (−0.66), 1998 (−0.82), and 1997 (−0.76).

The superposed epoch analysis—performed with the derived drought years by the SPEI—revealed similar drought responses of the trees at OGS and CPS (Fig. 4). The trees at both sites showed decreased growth values during drought years (0). In the first (1) and second (2) years following drought, growth was still significantly lower than the average growth of the time series. In the third year (3) after a drought event, the trees recovered sufficiently to resume tree ring growth. There were no significant differences in the growth during and after drought between green-OGS and paved-CPS. The younger trees at OGS exhibited a smaller growth decrease following the drought years than the older trees at CPS. The trees of paved-CPS had a stronger growth decline during the drought year. However, in the third and fourth years after a drought event, the older trees at CPS showed a better growth compared to the average growth of the time series and a greater recovery than the trees at OGS.

Analysis of the long-term growth of trees at both sites highlighted similar reaction patterns during drought regardless of differences in age and surface properties. The highly significant growth reductions in the second post-drought year at both sites might also be influenced by the drought year occurrence; the drought years 2014, 2003, and 1997 might have subsequent aftereffects of water stress and reduced tree growth, which increased the drought stress on the trees strongly, leading to the greatest growth drop afterwards.

Table 2 Calculated age, growth rate, basal area increment (BAI), mean sensitivity of growth, and expressed population signal (EPS) of *Tilia cordata* at Bordeaux Platz (open green square OGS) and Pariser Platz (completely paved square CPS) with standard deviation (SD) based on tree ring data

Site	Age [a]	Growth rate ± SD [mm year^{-1}]	BAI ± SD [mm^2 year^{-1}]	Mean sensitivity	EPS[a]
Green-OGS	43	5.0 ± 0.6	80.5 ± 57.4	0.5	0.9
Paved-CPS	95	2.6 ± 0.8	206.7 ± 149.5	0.4	0.9

[a] Based on the ring width index of tree ring chronologies for the common period, obtained by double detrending of the tree ring series

Table 3 Positive and negative pointer years detected by the year ring width of *Tilia cordata* at both sites and at Bordeaux Platz (open green square OGS) as well as Pariser Platz (completely paved square CPS) separately (italic years of CPS outside of the common time period of both sites)

Site	Positive	n	Negative	n
Both	2012, 2010, 2006, 2000, 1995	5	2014, 2011, 2009, 2005	4
Green-OGS	2002, 1992, 1990, 1987	4	1999, 1998, 1994, 1989	4
Paved-CPS	2013, 2004, 1989, *1965, 1950, 1947*	6	2015, 2003, 1997, *1941, 1933*	5

Intraannual growth patterns (2015)

All in all, the daily growth increment of *T. cordata* at two contrasting sites decreased over the summer. At OGS, the trees showed a steady increase in a daily diameter until mid-August. Then, growth of most trees started to decline, with tree no. 2 decreasing the most by 1.0 mm in diameter. Other trees such as nos. 1, 3, and 4 illustrated minor growth reduction. Only tree no. 5 grew slightly during summer. Compared to green-OGS, the trees at CPS exhibited significantly reduced growth. While the trees at OGS grew up to 2.5 mm until mid of August, the trees at CPS had only 0.4-mm diameter increment. Moreover, the growth patterns during the observed period are different at CPS, where all investigated trees had a distinct reduction in growth until mid (only tree no. 5) or end of September (rest of the trees). After initial diameter expansion, tree diameter contracted again during the summer up to 0.8 mm at the end of our investigation (Fig. 5).

Trees at both sites reacted similarly to microclimate (Fig. 6). Only soil matric potential, soil temperature, transpiration in September, and wind speed in August and September displayed contrary patterns in their relationships with growth at both sites. The vapor pressure deficit and the air temperature were negatively correlated with growth at both sites, with a very strong negative relationship throughout August, September, and October at OGS. However, the observed negative relationship was visible only in October at CPS. The amount of precipitation on the other hand was beneficial for tree growth, especially for the trees at OGS. Transpiration mostly had a negative correlation with tree growth, though in July and September both illustrated a positive relationship with growth at CPS, while in July transpiration showed a positive correlation with the tree growth at OGS. Additionally, the soil matric potential changed in its relationship with tree growth: In August, a less negative soil matric potential was beneficial for growth at both sites, while in September a positive relationship with growth was observed at OGS. In October, the soil matric potential was negatively correlated with the growth at both sites. Finally, higher soil temperature had a negative effect on tree growth during all 3 months at OGS, while soil temperature had a positive effect on growth at CPS in August. The following months also showed a negative correlation. In summary, all measured meteorological data except precipitation had a negative correlation with growth, with vapor pressure deficit, air temperature, transpiration, and soil matric potential illustrating the greatest influence ($r < -0.5$, $r^2 > 25$) on tree growth (Fig. 6 (i)).

A performed GAMM revealed a significantly lower interannual growth rate of the trees at CPS compared to OGS (Table 4). Moreover, there was a significant influence of the soil matric potential, precipitation, and transpiration on tree growth. The soil temperature, vapor pressure deficit, air temperature, and wind speed had no significant influence on growth in relation to the site differences and were consequently removed from the final model. The strongest negative influence had the site and the transpiration decreasing growth, while precipitation and the soil matric potential proved to be of positive influence on tree growth.

Fig. 2 Ring width index (RWI) of *Tilia cordata* at Bordeaux Platz (OGS, *solid line*) and Pariser Platz (CPS, *dashed line*) after double detrending (negative exponential function and 2/3 cubic smoothing spline)
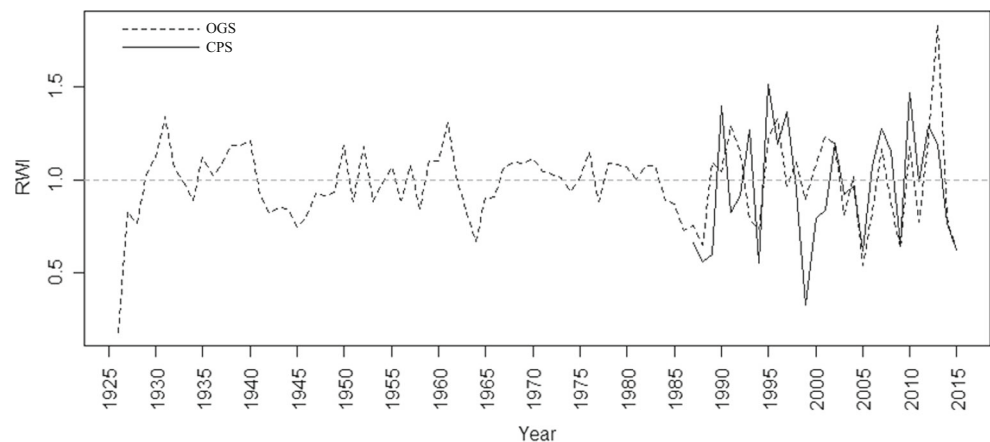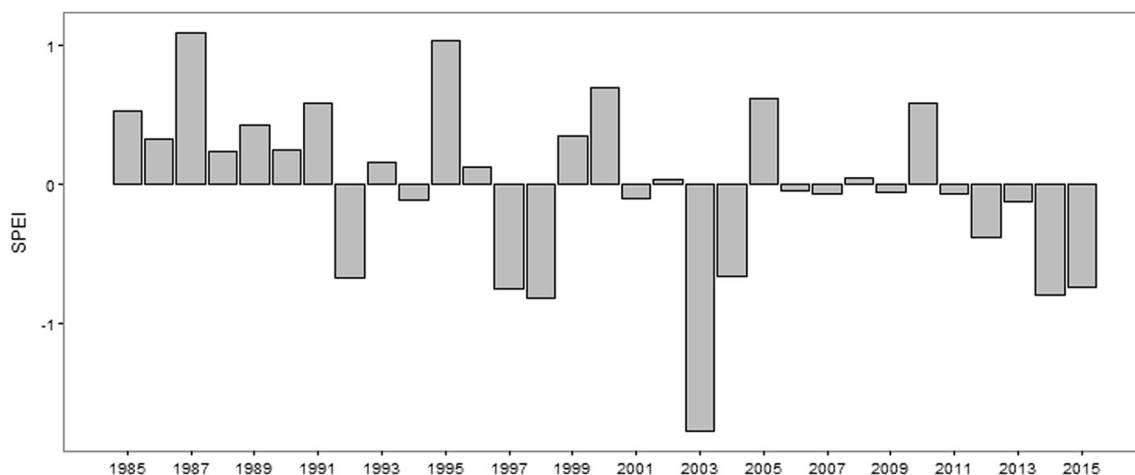
Fig. 3 Calculated standard precipitation-evapotranspiration index (SPEI) for Munich from 1985 to 2015 with a time scale of 4 months. *Bars > 0* represent positive SPEI values of years with a positive climatic water balance, and *bars < 0* represent negative SPEI values of years with a negative climatic water balance

Discussion

Structure of *T. cordata* at Bordeaux Platz and Pariser Platz

This study illustrated that growth patterns of *T. cordata* were highly influenced by the surrounding environment. The average tree growth during the severe drought year 2015 at the highly paved site Pariser Platz CPS was significantly lower than the growth of the trees at the more open, greener Bordeaux Platz OGS and confirmed the original hypothesis of reduced growth due to extreme environmental conditions associated with paving. This pattern of an overall greater growth of younger trees might also be influenced by the CPS trees being older (they were on average 52 years older), since age can induce greater DBH and crown dimensions. As a study of Ryan et al. (1997) showed, younger trees grow faster than older trees ("age-trend"), but age-related bias in ring increment was removed by detrending. Thus, the results

of the drought year analysis SEA were not influenced by differing age between the two sites.

As shown in Table 1, the investigated trees at CPS varied in their age and size development, even though they were planted in short distance of each other, which may be due to heterogeneous soils and microclimates, e.g., shading by buildings. Bühler et al. (2006) found similar patterns of varying size of established *T. cordata* trees in Copenhagen. However, the measured structural dimensions of *T. cordata* at both sites are in line with other studies about the growth of this species. For example, Moser et al. (2015) measured the growth and selected ecosystem services of *T. cordata* trees in Munich, especially analyzing the allometry based on dbh. The trees at CPS were similar to those measured by Moser et al. (2015). Due to being older, they represented the upper range of urban tree growth and tree structures. By contrast, younger trees at OGS had more uniform and slightly faster growth compared to the results of Moser et al. (2015). A comparison of the *T. cordata* structural dimensions with a study of Larsen and Kristoffersen
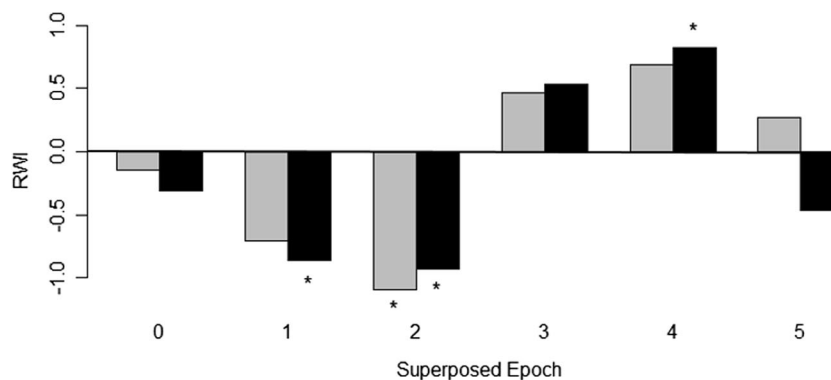

Fig. 4 Superposed epoch analysis of the ring width index (RWI) during drought years (0) and after drought (1–5) for *Tilia cordata* at Bordeaux Platz (OGS, *gray*) and Pariser Platz (CPS, *black*). Input drought years are 2015, 2014, 2004, 2003, 1998, 1997, and 1992. Marked columns (*asterisk*) are significantly different at $p < 0.05$
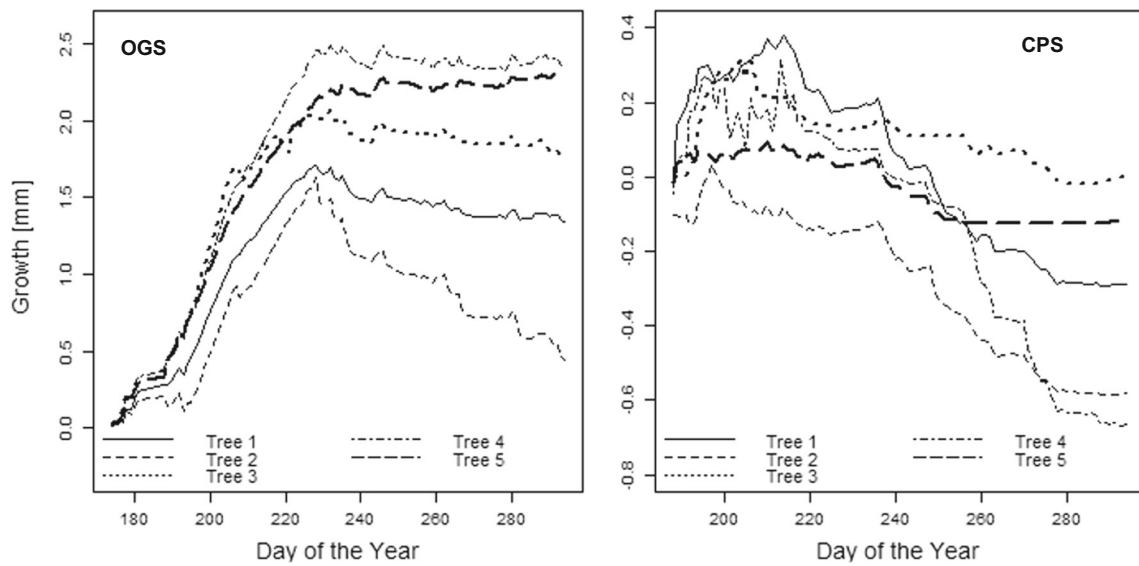
Fig. 5 Daily growth of the *Tilia cordata* trees at Bordeaux Platz (OGS, *left*) and Pariser Platz (CPS, *right*) during summer, 2015 (July, 1st to October, 21st, 2015)
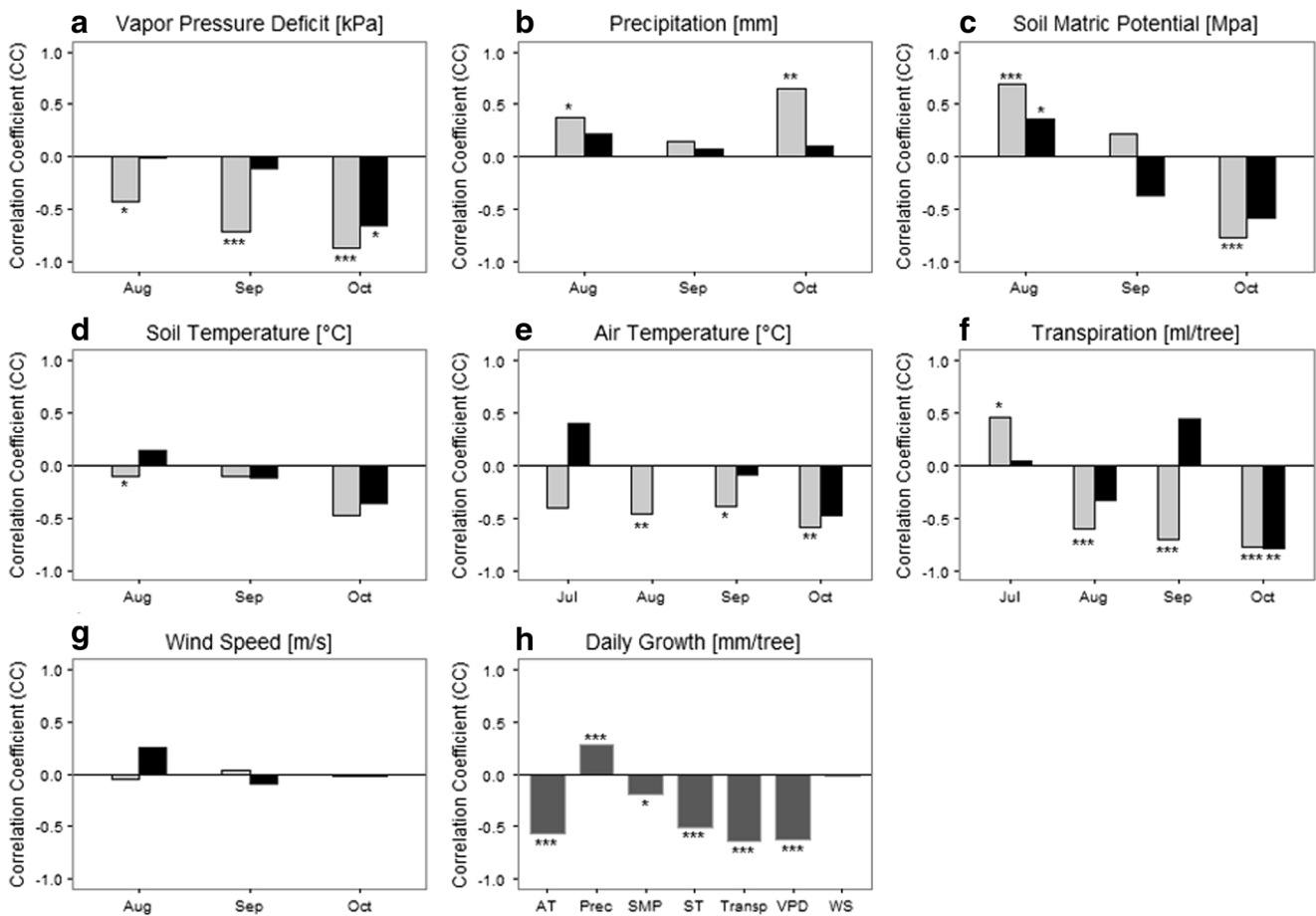

Fig. 6 Correlations between minimum daily growth and **a** vapor pressure deficit (*VPD*), **b** precipitation (*Prec*), **c** soil matric potential (*SMP*), **d** soil temperature (*ST*), **e** air temperature (*AT*), **f** transpiration (*Transp*), and **g** wind speed (*WS*) of *Tilia cordata* at Bordeaux Platz (OGS, *gray bars*) and Pariser Platz (CPS, *black bars*) in July, August, September, and October 2015, and **h** the correlations of measured meteorological data with growth at both sites together. <u>*Asterisks*</u> indicate a significant correlation (*at the $\alpha < 0.05$, **at the $\alpha < 0.01$, ***at an α-level < 0.001)

Table 4 Generalized additive mixed model (GAMM) on the mean daily growth rates of *Tilia cordata* at Bordeaux Platz (open green square OGS) and Pariser Platz (completely paved square CPS) from July to October 2015 of the form: daily growth [mm] = a + s(day, by site) + b × soil matric potential + c × precipitation + d × Transpiration

	Value ± SE	p
Intercept (a)	−0.03 ± 0.01	0.02
Site (s)	−0.01 ± 0.003	< 0.001
Soil matric potential (b)	0.01 ± 0.003	0.003
Precipitation (c)	0.002 ± 0.0002	< 0.001
Transpiration (d)	$-2.2 \times 10^{-7} \pm 1.0 \times 10^{-7}$	0.03
SD intercept (e)	0.003	–
ε	0.02	–

Levels of site: 2 (CPS and OGS)

SD standard deviation, *SE* standard error

(2002) in Copenhagen revealed that the measured trees at OGS had a similar dbh with a faster height growth, while the trees at CPS were smaller than those of the same age in Copenhagen. Less growth and structural dimensions of the CPS trees was likely induced by greater heat and drought stress due to surrounding paving, building proximity, small planting pits, and compacted soil that would limit rooting volume and uptake of soil water, reducing vitality and ultimately leading to reduced growth as shown by Nielsen et al. (2007).

Interannual and intraannual growth patterns, climate-growth relationships

However, Nielsen et al. (2007) did not analyze the growth patterns during drought, which may limit growth even further. In our study, we measured the diameter increment of ten *T. cordata* trees at two contrasting sites in high temporal resolution (every 5 min) during the hot and dry summer of 2015. Overall, the measured trees showed increased diameter growth until the beginning of August, with the trees at the highly paved site CPS exhibiting a growth reduction several days earlier than those at the more open and greener OGS. When comparing both sites, the effect of shrinkage due to extensive drought was observed for CPS later in the season, though not at OGS. Reduction in diameter occurs when tree transpiration exceeds availability of stored intercellular and soil water uptake (Sjöman et al., 2015). If this imbalance continues, tree diameter decrease and further decline in growth may occur as a combination of influences like limited water supply, loss of hydraulic conductance, reduced photosynthesis, restricted soil and rooting volume, disruption in soil hydrological processes, and climate. Further, impermeable surfaces and compacted soil can accelerate water deficits (Sieghardt et al., 2005; Morgenroth and Visser, 2011; Sjöman et al., 2015). Physiological differences in response

to drought may be due to different site conditions. The dendrochronological analysis showed that more negative pointer years were found at the paved site (9 at CPS compared to 8 at OGS), likely as a result of their greater age (Ryan et al., 1997). However, more positive pointer years were found for OGS in the common time period of both sites (8 at CPS to 9 at OGS). SEA analysis revealed similar patterns in growth during and after drought at CPS and OGS. Significant increment growth reductions were found in the years after a drought event. Slight differences were revealed in the severity of the growth reductions and the following recovery, with the highly paved-CPS exhibiting greater growth decreases after drought though better recovery. This might be due to the higher tree age at CPS, since older trees can recover better from drought events (Lloret et al., 2011).

The patterns of growth reductions after drought events can be explained with the evident anisohydric water stress behavior of *T. cordata*. Anisohydric species allow their leaf water potential to decrease during drought by sustaining a relatively high stomatal conductance and thus carbon assimilation (Klein, 2014; Roman et al., 2015). Therefore, growth may be reduced as a consequence in the years following drought events (Pretzsch et al., 2014; Río et al., 2014). While during the drought event, no immediate growth reductions would occur, minimal stomatal closure means high transpiration rates despite soil drying, leading to a greater risk of cavitation and disruptions in xylem water management (McDowell et al., 2008; Roman et al., 2015), decreasing growth and vitality in subsequent years. High atmospheric demand along with high transpiration rates due to a limited soil moisture availability might also cause the observed shrinkage of trees at CPS as a consequence of the drought year 2015 and previous drought years like 2014.

Differences in 2015 growth patterns found by dendrometer were likely caused by site differences in terms of microclimate. Most importantly the study illustrated the negative influence of high temperatures, less water availability and transpiration on tree growth, especially during drought years. All measured meteorological data except precipitation had a negative influence on tree growth, while higher air and soil temperatures, a greater vapor pressure deficit as well as higher transpiration resulted in reduced growth during summer. These findings are in line with the mixed model results, a reduced amount of precipitation results in less water availability in the soil, leading to a reduced soil matric potential. Increased air and soil temperatures induce higher vapor pressure deficit (Kirschbaum, 2004) resulting in higher transpiration and hence evapotranspirational cooling (Rahman et al., 2014), depleting the intracellular stored water. The relationship between growth and meteorological variables, in particular transpiration, was also likely due to the anisohydric character of *T. cordata*. High atmospheric demand translates to high transpiration rates in anisohydric species, resulting in

greater soil water depletion, water stress, and stem shrinkage that ultimately reduce increment growth (Marsal et al., 2002; Scoffoni et al., 2014). Albeit, trees with a higher transpiration rate should also have a higher girth and are expected to have greater cooling abilities, since trees with higher girth usually have a greater sapwood area and more sap flow to support more leaf area (Rahman et al., 2014; Moser et al., 2015).

Aggressive anisohydric water use behavior might provide greater overall evaporate cooling and thermal comfort to mitigate the effects of climate change. However, our study suggests that added cooling during a hot, dry year may come at the cost of reduced growth in subsequent years. This makes *T. cordata* a not very suitable urban tree species under hotter, drier conditions, especially at paved, impervious sites like CPS, where irrigation might be needed to meet transpiration needs and sustain evaporative cooling of anisohydric species such as *T. cordata*. At the limits of extreme drought, such water use behavior could prove unsuitable, increasing the risk of damage to tree health and loss of canopy (Kolb and Stone, 2000; Klein, 2014). Thus, in the context of a hotter, drier climate, species with an isohydric water stress response might be a more suitable choice for harsh sites with reduced water availability.

Conclusions

In conclusion, the conducted study could display how the growth of *T. cordata* at two contrasting sites was influenced by the surrounding environment in terms of the site conditions soil, size of planting pits, and meteorological variables like precipitation and temperature. Since the urban environment is very heterogeneous, even sites in short distance (like green-OGS and paved-CPS) can vary tremendously. Those site differences and the severe drought year 2015 caused a decrease in the growth of the measured trees at both sites; however, the *T. cordata* trees at CPS suffered significantly more to the degree of the shrinkage of tree girth in summer. This was very likely induced by a negative water balance due to insufficient water supply consequently high negative soil matric potential and following high water loss through transpiration. Due to the anisohydric water stress response of this species, *T. cordata* can provide high rates of cooling even during drought years, however, which can cause high growth decreases afterwards. In the future, tree species which achieve a better balance between growth, transpiration, and hence evaporative cooling should be preferred. The observed patterns of tree behavior during and after drought events were mainly caused by species traits and also influenced by the environment. Though the present study showed the negative influence of highly paved sites with related problems like less water availability and rooting space on tree growth, especially during drought years, there are still knowledge gaps

concerning other issues affecting growth, e.g., effects of the growing media and planting methods, irrigation, as well as the specific microclimate environment at the tree site. There is an increasing demand for future studies on these influences to gain more expertise for sustainable tree planting, particularly at difficult sites to ensure healthy, well-grown trees, providing ecosystem services such as evaporative cooling also under future climate change conditions.

Compliance with ethical standards

Conflict of interest The authors declare that they have no conflict of interest.

References

Akbari H, Pomerantz M, Taha H (2001) Cool surfaces and shade trees to reduce energy use and improve air quality in urban areas. Sol Energy 70:295310

Allen CD, Macalady AK, Chenchouni H, Bachelet D, McDowell N, Vennetier M, Kitzberger T, Rigling A, Breshears DD, Hogg EH, Gonzalez P, Fensham R, Zhang Z, Castro J, Demidova N, Lim J-H, Allard G, Running SW, Semerci A, Cobb N (2010) A global overview of drought and heat-induced tree mortality reveals emerging climate change risks for forests. For Ecol Manag 259:660–684

Allen RG, Pereira LS, Raes D, Smith M (1998) Crop evapotranspiration—guidelines for computing crop water requirements—FAO irrigation and drainage paper. FAO. Rome 56

Arndt SK, Wanek W, Clifford SC, Popp M (2000) Contrasting adaptations to drought stress in field-grown *Ziziphus mauritiana* and *Prunus persica* trees: water relations, osmotic adjustment and carbon isotope composition. Aust J Plant Physiol 27:985–996

Briffa KR, Jones PD (1990) Basic chronology statistics and assessment. In: Cook ER, Kairiukstis LA (eds) Methods of dendrochronology: applications in the environmental sciences. International Institute for Applied Systems Analysis. Kluwer Academic Publishers, Boston, pp. 137–152

Bühler O, Kristoffersen P, Larsen SU (2007) Growth of street trees in Copenhagen with emphasis on the effect of different establishment concepts. Arboric Urban For 5:330–337

Bühler O, Nielsen CN, Kristoffersen P (2006) Growth and phenology of established *Tilia cordata* street trees in response to different irrigation regimes. Arboric Urban For 32:3–9

Bunn A, Korpela M, Biondi F, Campelo F, Mérian P, Qeadan F, Zang C, Buras A, Cecile J, Mudelsee M, Schulz M, (2015) Package 'dplR'. Dendrochronology Program Library in R. In.

Bush SE, Pataki DE, Hultine KR, West AG, Sperry JS, Ehleringer JR (2008) Wood anatomy constrains stomatal responses to atmospheric vapor pressure deficit in irrigated, urban trees. Oecologia 156:13–20

Chen L, Zhang Z, Li Z, Tang J, Caldwell P, Zhang W (2011) Biophysical control of whole tree transpiration under an urban environment in northern China. J Hydrol 402:388–400

Clark JR, Kjelgren R (1990) Water as a limiting factor in the developement of urban trees. J Arboric 16:203–208

Comstock JP, Mahall BE (1985) Drought and changes in leaf orientation for two California chaparral shrubs: *Ceanothus megacarpus* and *Ceanothus crassifolius*. Oecologia 65:531–535

Day SD, Bassuk NL, van Es H (1995) Effects of four compaction remediation methods for landscape trees on soil aeration, mechanical impedance and tree establishment. J Arboric 22:144–150

Day SD, Wiseman PE, Dickinson SB, Harris JR (2010) Contemporary concepts of root system architecture of urban trees. Arboric Urban For 4:149–157

Dimoudi A, Nikolopoulou M (2003) Vegetation in the urban environment: microclimatic analysis and benefits. Energy Build 35:69–76

Dobbertin M (2005) Tree growth as indicator of tree vitality and of tree reaction to environmental stress: a review. Eur J For Res 124:319–333

Dobbs C, Kendal D, Nitschke CR (2014) Multiple ecosystem services and disservices of the urban forest establishing their connections with landscape structure and sociodemographics. Ecol Indic 43:44–55

Drew DM, Downes GM (2009) The use of precision dendrometers in research on daily stem size and wood property variation: a review. Dendrochronologia 27:159–172

DWD (2016) Deutscher Wetterdienst. Available online: http://www.dwd.de

Elmi AA, West CP (1995) Endophyte infection effects on stomatal conductance, osmotic adjustment and drought recovery of tall fescue. New Phytol 131:61–67

Gallé A, Haldimann P, Feller U (2007) Photosynthetic performance and water relations in young pubescent oak (*Quercus pubescens*) trees during drought stress and recovery. The New phytologist 174:799–810

Gill S, Handley J, Ennos R, Pauleit S (2007) Adapting cities for climate change: the role of the green infrastructure. Build Environ 33:115–133

Gillner S, Bräuning A, Roloff A (2014) Dendrochronological analysis of urban trees: climatic response and impact of drought on frequently used tree species. Trees 28:1079–1093

Gómez-Muñoz VM, Porta-Gándara MA, Fernández JL (2010) Effect of tree shades in urban planning in hot-arid climatic regions. Landsc Urban Plan 94:149–157

Gregg JW, Jones CG, Dawson TE (2003) Urbanization effects on tree growth in the vicinity of New York City. Nature 424:183–187

Hodge SJ, Boswell R (1993) A study of the relationship between site conditions and urban tree growth. J Arboric 19:358–367

IPCC (2007) Climate change 2007: the physical science basis. Contribution of working group I to the fourth assessment report of the intergovernmental panel on climate change. Cambridge University Press, Cambridge and New York

Kim HH (1992) Urban Heat Island. Intl J Remote Sensing 13:2319–2336

Kirschbaum MUF (2004) Direct and indirect climate change effects on photosynthesis and transpiration. Plant Biol 6:242–253

Kjelgren RK, Clark JR (1992) Microclimates and tree growth in tree urban spaces. J Environ Hortic 10:139–145

Kjelgren RK, Montague T (1998) Urban tree transpiration over turf and asphalt surfaces. Atmos Environ 32:35–41

Klein T (2014) The variability of stomatal sensitivity to leaf water potential across tree species indicates a continuum between isohydric and anisohydric behaviours. Funct Ecol 28:1313–1320

Ko Y, Lee J-H, McPherson EG, Roman LA (2015) Factors affecting long-term mortality of residential shade trees: evidence from Sacramento, California. Urban For Urban Greening 14:500–507

Kolb TE, Stone JE (2000) Differences in leaf gas exchange and water relations among species and tree sizes in an Arizona pine-oak forest. Tree Physiol 20:1–12

Larsen FK, Kristoffersen P (2002) Tilia's physical dimensions over time. J Arboric 28:209–214

Littell JS, Peterson DL, Tjoelker M (2008) Douglas-fir growth in mountain ecosystems: water limits tree growth from stand to region. Ecol Monogr 78:349–368

Liu F, Stützel H (2004) Biomass partitioning, specific leaf area, and water use efficiency of vegetable amaranth (Amaranthus spp.) in response to drought stress. Sci Hortic 102:15–27

Lloret F, Keeling EG, Sala A (2011) Components of tree resilience: effects of successive low-growth episodes in old ponderosa pine forests. Oikos 120:1909–1920

Lough JM, Fritts HC (1987) An assessment of the possible effects of volcanic eruptions on north American climate using tree-ring data, 1602 to 1900 a.D. Clim Chang 10:219–239

Mäkinen H, Seo J-W, Nöjd P, Schmitt U, Jalkanen R (2008) Seasonal dynamics of wood formation: a comparison between pinning, microcoring and dendrometer measurements. Eur J For Res 127:235–245

Marsal J, Gelly M, Mata M, Arbonés A, Rufat J, Girona J (2002) Phenology and drought affects the relationship between daily trunk shrinkage and midday stem water potential of peach trees. J Hortic Sci Biotechnol 77:411–417

McDowell N, Pockman WT, Allen CD, Breshears DD, Cobb N, Kolb T, Plaut J, Sperry J, West A, Williams DG, Yepez EA (2008) Mechanisms of plant survival and mortality during drought: why do some plants survive while others succumb to drought? The New phytologist 178:719–739

McPherson EG, Nowak DJ, Heisler G, Grimmond S, Souch C, Grant R, Rowntree RA (1997) Quantifying urban forest structure, function, and value: the Chicago urban Forest climate project. Urban Ecosyst 1:49–61

Mérian P, Lebourgeois F (2011) Size-mediated climate–growth relationships in temperate forests: a multi-species analysis. For Ecol Manag 261:1382–1391

Miller JB (1967) A formula for average foliage density. Aust J Bot 15:141–144

Morgenroth J, Buchan GD (2009) Soil moisture and aeration beneath pervious and impervious pavements. Arboric Urban For 35:135–141

Morgenroth J, Visser R (2011) Aboveground growth response of *Platanus orientalis* to porous pavements. Arboric Urban For 37:1–5

Moser A, Rötzer T, Pauleit S, Pretzsch H (2015) Structure and ecosystem services of small-leaved lime (*Tilia cordata* mill.) and black locust (*Robinia pseudoacacia* L.) in urban environments. Urban For Urban Greening 14:1110–1121

Moser A, Rötzer T, Pauleit S, Pretzsch H (2016) The urban environment can modify drought stress of small-leaved lime (*Tilia cordata* mill.) and black locust (*Robinia pseudoacacia* L.). Forests 7:71

Nielsen CN, Bühler O, Kristoffersen P (2007) Soil water dynamics and growth of street and park trees. Arboric Urban For 33:231–245

Nowak DJ, Crane DE (2002) Carbon storage and sequestration by urban trees in the USA. Environ Pollut 116:381–389

Nowak DJ, McBride J, Beatty R (1990) Newly planted street tree growth and mortality. J Arboric 27:306–317

Orwig DA, Abrams DA (1997) Variation in radial growth responses to drought among species, site, and canopy strata. Trees 11:474–484

Pauleit S, Jones N, Garcia-Marin G, Garcia-Valdecantos J-L, Rivière LM, Vidal-Beaudet L, Bodson M, Randrup TB (2002) Tree establishment practice in towns and cities—results from a European survey. Urban For Urban Greening 1:83–96

Pongracz R, Bartholy J, Dezsoe Z (2010) Application of remotely sensed thermal information to urban climatology of central European cities. Phys Chem Earth 35:95–99

Pretzsch H, Dieler J (2011) The dependency of the size-growth relationship of Norway spruce (*Picea abies* [L.] Karst.) and European beech (*Fagus sylvatica* [L.]) in forest stands on long-term size conditions, drought events, and ozone stress. Trees 25:355–369

Pretzsch H, Rötzer T, Matyssek R, Grams TEE, Häberle K-H, Pritsch K, Kerner R, Munch J-C (2014) Mixed Norway spruce (*Picea abies* [L.] Karst) and European beech (*Fagus sylvatica* [L.]) stands under drought: from reaction pattern to mechanism. Trees 28:1305–1321

R Core Team, 2014. R: A language and environment for statistical computing. R Foundation for Statistical Computing. In, Vienna, Austria.

Radoglou K, Dobrowolska D, Spyroglou G, Nicolescu V-N (2009) A review on the ecology and silviculture of limes (*Tilia cordata* mill., *Tilia platyphyllos* Scop. And *Tilia tormentosa* Moench.) in Europe. Die. Bodenkultur 60:9–19

Rahman MA, Armson D, Ennos AR (2014) Effect of urbanization and climate change in the rooting zone on the growth and physiology of *Pyrus calleryana*. Urban For Urban Greening 13:325–335

Rahman MA, Armson D, Ennos AR (2015) A comparison of the growth and cooling effectiveness of five commonly planted urban tree species. Urban Ecosyst 18:371–389

Rahman MA, Moser A, Rötzer T, Pauleit S (2017) Microclimatic differences and their influence on transpirational cooling of *Tilia cordata* in two contrasting street canyons in Munich, Germany. Agric For Meteorol 232:443–456

Rahman MA, Stringer P, Ennos AR (2013) Effect of pit design and soil composition on performance of *Pyrus calleryana* street trees in the establishment period. Arboric Urban For 39:256–266

Rhoades RW, Stipes RJ (1999) Growth of trees on Virgina tech campus in response to various factors. J Arboric 25:211–217

Rinn F (2005) TSAP reference manual. Rinntech, Heidelberg, http://www.rinntech.com/

Rinn Tech (2010) TSAP-Win: time series analysis and presentation for dendrochronology and related applications. In, Heidelberg, Germany.

Río MD, Schütze G, Pretzsch H (2014) Temporal variation of competition and facilitation in mixed species forests in Central Europe. Plant Biol 16:166–176

Roman DT, Novick KA, Brzostek ER, Dragoni D, Rahman F, Phillips RP (2015) The role of isohydric and anisohydric species in determining ecosystem-scale response to severe drought. Oecologia 179:641

Rötzer, T., Seifert, T., Gayler, S., Priesack, E., Pretzsch, H., 2012. Effects of Stress and Defence Allocation on Tree Growth: Simulation Results at the Individual and Stand Level. In: al., R.M.e. (Ed.), Growth and Defence in Plants, Ecological Studies. Springer-Verlag, Berlin Heidelberg, pp. 401–432.

Ryan MG, Binkley D, Fownes JH (1997) Age-related decline in Forest productivity: pattern and process. Adv Ecol Res 27:213–262

Sandquist DR, Ehleringer JR (1998) Intraspecific variation of drought adaptation in brittlebush: leaf pubescence and timing of leaf loss vary with rainfall. Oecologia 113:162–169

Scoffoni C, Vuong C, Diep S, Cochard H, Sack L (2014) Leaf shrinkage with dehydration: coordination with hydraulic vulnerability and drought tolerance. Plant Physiol 164:1772–1788

Shashua-Bar L, Hoffman ME (2003) Geometry and orientation aspects in passive cooling of canyon streets with trees. Energy Build 35:61–68

Sieghardt M, Mursch-Radlgruber E, Paoletti E, Couenberg E, Dimitrakopoulus A, Rego F, Hatzistathis A, Randrup TB (2005) The abiotic urban environment: impact of urban growing conditions on urban vegetation. In: Konijnendijk C, Nilsson K, Randrup T, Schipperijn J (eds) Urban forests and trees: a reference book. Springer Berlin Heidelberg, Berlin, pp. 281–323

Sjöman H, Hirons AD, Bassuk NL (2015) Urban forest resilience through tree selection−Variation in drought tolerance in *Acer*. Urban For Urban Greening 14:858–865

Speer JH (2012) Fundamentals of tree-ring research. The University of Arizona Press, Tucson

Tyree MT, Cochard H, Cruiziat P, Sinclair B, Ameglio T (1993) Drought-induced leaf shedding in walnut: evidence for vulnerability segmentation. Plant Cell Environ 16:879–882

Tyrväinen L, Pauleit S, Seeland K, Vries S (2005) Benefits and uses of urban forests and trees. In: Konijnendijk C, Nilsson K, Randrup T, Schipperijn J (eds) Urban forests and trees: a reference book. Springer Berlin Heidelberg, Berlin, Heidelberg, pp. 81–114

Vicente-Serrano SM, Beguería S, López-Moreno JI (2010) A Multiscalar drought index sensitive to global warming: the standardized precipitation evapotranspiration index. J Clim 23:1696–1718

Welles JM, Norman JM (1991) Instrument for indirect measurement of canopy architecture. Agron J 83:818–825

Werner C, Correia O, Beyschlag W (1999) Two different strategies of Mediterranean macchia plants to avoid photoinhibitory damage by excessive radiation levels during summer drought. Acta Oecol 20:15–23

Wigley TML, Briffa KR, Jones PD (1984) On the average value of correlated time series, with applications in dendroclimatology and hydrometeorology. J Climate Appl Meteor 23:201–213

Williams AP, Allen CD, Macalady AK, Griffin D, Woodhouse CA, Meko DM, Swetnam TW, Rauscher SA, Seager R, Grissino-Mayer HD, Dean JS, Cook ER, Gangodagamage C, Cai M, McDowell NG (2013) Temperature as a potent driver of regional forest drought stress and tree mortality. Nat Clim Chang 3:292–297

Yoon TK, Park C-W, Lee SJ, Ko S, Kim KN, Son Y, Lee K-H, Oh S, Lee W-K, Son Y (2013) Allometric equations for estimating the aboveground volume of five common urban street tree species in Daegu, Korea. Urban For Urban Greening 12:344–349

Zhao M, Running SW (2010) Drought-induced reduction in global terrestrial net primary production from 2000 through 2009. Science 329:940–943